Carrier dynamics in type-II GaSb/GaAs quantum dots

F. Hatami, M. Grundmann, N. N. Ledentsov,* F. Heinrichsdorff, R. Heitz, J. Böhrer, and D. Bimberg
Institut für Festkörperphysik, Technische Universität Berlin, D-10623 Berlin, Germany

S. S. Ruvimov† and P. Werner
Max-Planck-Institut für Mikrostrukturphysik, Weinberg 2, D-06120 Halle, Germany

V. M. Ustinov, P. S. Kop'ev, and Zh. I. Alferov
A. F. Ioffe Physical-Technical Institute, 194021 St. Petersburg, Russia
(Received 10 June 1997)

The optical properties and dynamics of charge carriers in self-organized arrays of type-II (staggered band lineup) GaSb/GaAs quantum dots are studied. Interband absorption from type-II quantum dots is evidenced; the energetic positions of quantum dot absorption peaks coincide with those apparent in photoluminescence spectra. (Sb,As) intermixing with an antimony diffusion length of about 1 nm is found to make an important contribution to the observed transition energies. Dipole layer formation and quantum dot state filling contribute to the luminescence blueshift with increasing excitation density. The recombination rate of electrons with localized holes drastically depends on the average carrier density. When several carriers are localized at each dot, decay time constants around 5 ns, quite similar to type-I systems, are observed. Individual, spatially indirect excitons decay with much larger time constants close to 1 μs. The decay time of quantum dot luminescence is independent of the temperature in the measured range $T \leqslant 65$ K as expected for zero-dimensional excitons. [S0163-1829(98)04907-8]

I. INTRODUCTION

Using the coherent island Stranski-Krastanov growth mode dense arrays of self-organized quantum dots can be fabricated in numerous material systems. Most research is devoted currently to the $In_xGa_{1-x}As/Al_yGa_{1-y}As$ system with the aim of application in laser devices, the first being reported in Ref. 1. It is expected that the incorporation of antimony compounds will lead to usable quantum dots (QD) luminescence in the wavelength range well above 1.1 μm on GaAs substrates. The growth of pseudomorphic GaSb films on GaAs using metal-organic vapor deposition was reported in Ref. 2; above a critical thickness of 1.5 nm-large (>100 nm) elastically relaxed islands were observed. Formation of coherent dots in molecular-beam epitaxy (MBE) was reported in Ref. 3 and evidenced by transmission electron microscopy (TEM) images. Similar results were obtained in Ref. 4, also using scanning tunneling microscopy. Luminescence results have been reported for 22,[3] 28,[5] and 40–60 nm (Ref. 6) GaSb, 50 nm-diam InSb and 56 nm-diam AlSb [Ref. 5] quantum dots on GaAs. InSb dots were also created on InP substrates.[7] Recent experimental investigations comprise the determination of phonon energies[8] and local conduction-band offset[9] for GaSb/GaAs quantum dots.

(In,Ga,Al)Sb/GaAs heterostructures exhibit a type-II (staggered) band lineup featuring recombination from spatially indirect excitons and are thus electronically fundamentally different from their well-known As-containing type-I counterparts. A dramatic reduction of exciton oscillator strength is theoretically expected.[10] However, studies of the fundamental optical properties of such spatially indirect quantum dot excitons are scarce in the literature. Here, we will report absorption and recombination dynamics of type-II quantum dots. In Ref. 11 the recombination dynamics of carriers in samples containing GaSb quantum dots of 80 nm-diameter and 10 nm height has been investigated. The position of the QD luminescence between 1.35 and 1.4 eV (Ref. 11) appears, compared to that from our structures and those in Ref. 6, to be rather high and corresponds to the transition of a thin 0.3 nm GaSb/GaAs quantum well in our samples. Although strong Sb-As intermixing is observed in our dots, as is evidenced in detail below, luminescence from 22 nm-diam GaSb(As) QD's is observed at much lower energy close to 1.1 eV. We will show in this work that this transition exhibits a slow time constant (of about 0.6 μs) at low carrier density, which we attribute to the recombination of individual spatially indirect excitons at QD's.

II. GROWTH AND CHARACTERIZATION

Samples were grown by elemental source MBE on semi-insulating GaAs (100) substrates using a RIBER-32 MBE machine. Growth rates were 0.8 μm/h for both GaAs and GaSb. Arsenic and antimony vapor pressures were $(2-3)\times10^{-6}$ Torr. After oxide desorption, a 0.5 μm-thick GaAs buffer was grown at 600 °C followed by a short-period $GaAs/Al_{0.4}Ga_{0.6}As$ (2 nm/2 nm) superlattice with a total thickness of 20 and 5 nm GaAs. Subsequently, the growth was interrupted until the substrate had cooled down to 470 °C. Then the surface was exposed to an Sb flux, leading to the formation of a GaSb layer. We find that 10- and 30-s growth interruption under an Sb flux results in the formation of 1- and 2- ML-thick GaSb layers, respectively, (1 ML$\approx$0.3 nm). Further increase in GaSb thickness is accomplished by additionally opening the Ga shutter. The resulting structure is covered by a 5-nm-thick GaAs layer and

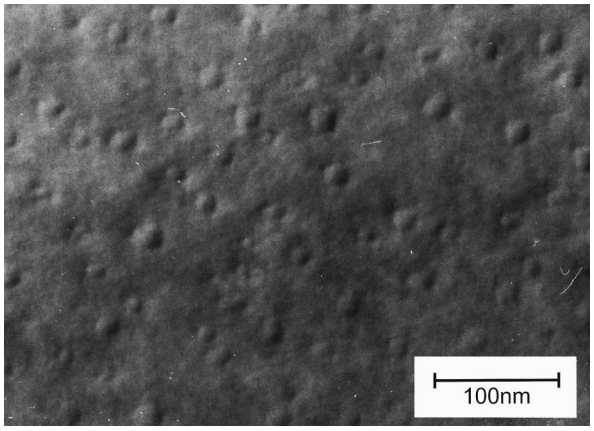

FIG. 1. Weak beam plan view TEM image of GaSb/GaAs quantum dots for 1.2 nm nominal GaSb deposition.

another superlattice. The GaAs quantum well and the superlattices are intended to prevent nonequilibrium carrier capture by surface-induced states and by deep centers in the GaAs:Cr semi-insulating substrate.

Plan view TEM studies are carried out in a high voltage JEOL JEM 1000 microscope operated at 1 MV. Photoluminescence (PL) was excited using the 514.5-nm line of an Ar^+ laser. The PL studies were performed in the temperature range of 2–300 K and an intensity range of $0.01-500\ \mathrm{W\,cm^{-2}}$ on 0.3-, 0.6-, 0.75-, and 0.9-nm GaSb quantum wells and GaSb QD's originating from deposition of 1.2-nm GaSb. Photoluminescence excitation (PLE) spectroscopy was performed at 2 K using a tungsten halogen lamp as excitation source. The light was dispersed by a 0.35-m double monochromator, analyzed with a double prism monochromator, and detected using a liquid-N_2-cooled Ge *p-i-n* diode with a total spectral resolution of 20 meV. Calorimetric absorption spectroscopy[12] was carried out at a base temperature of 500 mK. Time-resolved cathodoluminescence[13] (CL) was performed using an excitation voltage of 15 kV and a beam current of 6 nA with long excitation pulses of about 160 ns to create an equilibrium situation. Due to the slow time constants involved a low repetition rate of about 200 kHz was chosen. The CL was detected with a total time resolution of about 500 ps using a photomultiplier with *S*1 characteristics.

III. RESULTS AND DISCUSSION

A. Structural characterization

A weak-beam TEM image of the 1.2-nm GaSb sample is shown in Fig. 1. The contrast is partly due to strain fields. The in-plane projection of the quantum dot shape appears rectangular with rounder edges compared to that found for InAs/GaAs quantum dots.[14] Some additional contrast can be seen in TEM images due to the two-dimensional wetting layer resolved in between the GaSb dots. A statistical analysis of the size and shape of about 10^2 dots is shown in Fig. 2. The density of the dots is approximately $4\times10^{10}\ \mathrm{cm^{-2}}$. Most of the dots have a slightly asymmetric base shape. The dots exhibit an average lateral size $L=\sqrt{ab}$ of 22 nm with a standard deviation σ_L of 4.2 nm, a and b being the axes of the dots in the $\langle 100\rangle$ and $\langle 010\rangle$ directions, respectively. The

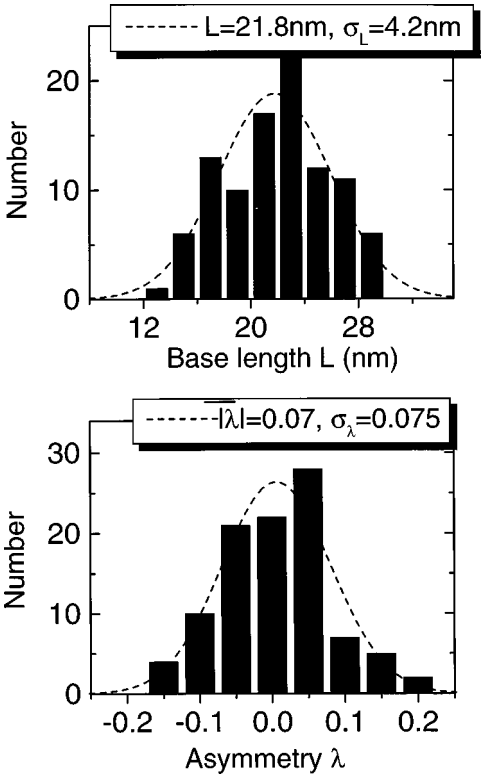

FIG. 2. Histogram of lateral size and asymmetry of quantum dots. The dashed lines show the corresponding Gaussian fits.

relative standard deviation $\sigma_L/\overline{L}$ is 19%. The asymmetry $\lambda=(a-b)/(a+b)$ has an average value of $\overline{|\lambda|}\approx0.07$.

B. Absorption

In order to study the electronic level structure of the dots we performed calorimetric absorption spectroscopy. In Fig. 3 we depict the calorimetric absorption spectrum of the 1.2-nm GaSb sample at 500 mK and the PL spectrum at 2 K and $0.05\ \mathrm{W\,cm^{-2}}$. The line at 1.23 eV in the PL spectrum is attributed to the heavy-hole electron ground-state (e_0,hh_0) transition in the wetting layer because it coincides with the energetic position of luminescence from GaSb quantum wells upon deposition of slightly smaller GaSb amount (0.9 nm, see Sec. III C). The second broad PL line at 1.09 eV coincides with the observed radiative recombination between the heavy holes confined in the GaSb quantum dots and two-dimensional electrons in the GaAs layer.[3,6] Similar to type-I quantum dots,[15] the energy positions of absorption and luminescence peaks of the quantum dots coincide. We observe at least one additional excited-state absorption peak at 1.16 eV between the QD ground-state absorption and the wetting-layer (WL) transition at 1.23 eV, which cannot yet clearly be assigned to a particular transition. Though the base length of about 22 nm is the smallest reported so far for GaSb quantum dots, it is relatively large and strong lateral confinement is not expected. An effective-mass calculation using biaxial strain for the rather flat dot geometry and a heavy-hole mass $m_{\mathrm{hh}}=0.28\ m_0$ (Ref. 16) indicates a heavy-hole sublevel separation due to the lateral confinement of about 7 meV. We speculate that the observed excited-state (QD*) is due to the quantization in the quantum dot along the growth direction.

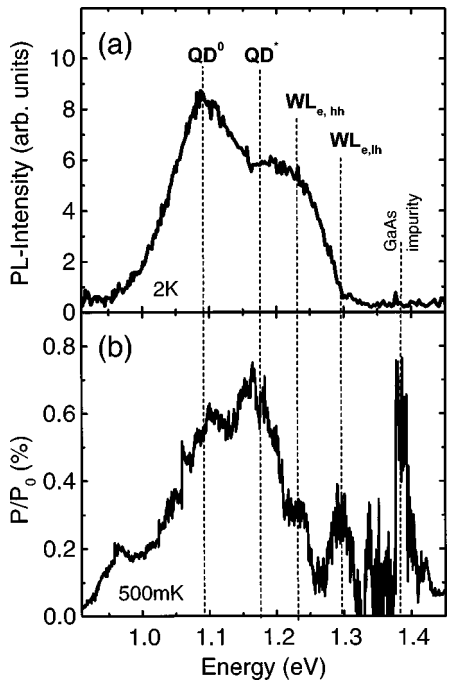

FIG. 3. (a) Calorimetric absorption spectrum ($T=500$ mK) and (b) low excitation density ($D=0.05$ W/cm^2) photoluminescence spectrum ($T=2$ K) of the 1.2-nm GaSb sample containing QD's.

C. PL and PLE

In Fig. 4 we show again the PL spectrum of the 1.2-nm GaSb sample containing quantum dots. For comparison, the spectra of three GaSb/GaAs structures with nominal average GaSb layer thicknesses of 0.3, 0.75, and 0.9 nm are depicted. Their luminescence is a single, intense, and relatively narrow peak due to heavy-hole electron transition in GaSb/GaAs type-II quantum wells.[17] The full width at half maximum (FWHM) for the 0.3- and 0.75-nm GaSb quantum wells is about 20 meV and for 0.9-nm GaSb quantum well about 50 meV. Formation of the GaSb dots results in a profound modification of the PL spectra. For the 1.2-nm GaSb sample we observe two PL lines due to heavy holes at different energies in the wetting layer and in the quantum dots. The

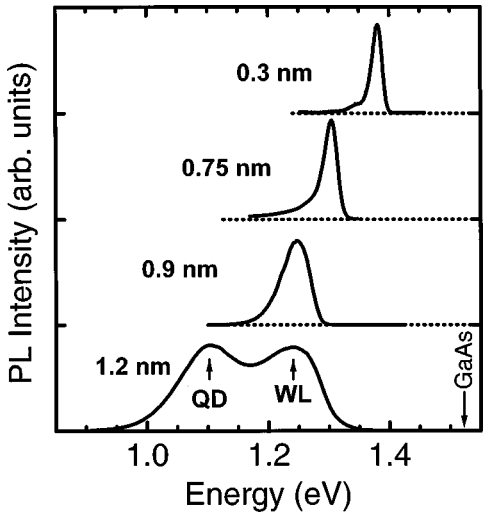

FIG. 4. Photoluminescence spectra ($D=5$ W/cm^2, $T=2$ K) of samples with different GaSb layer thickness.

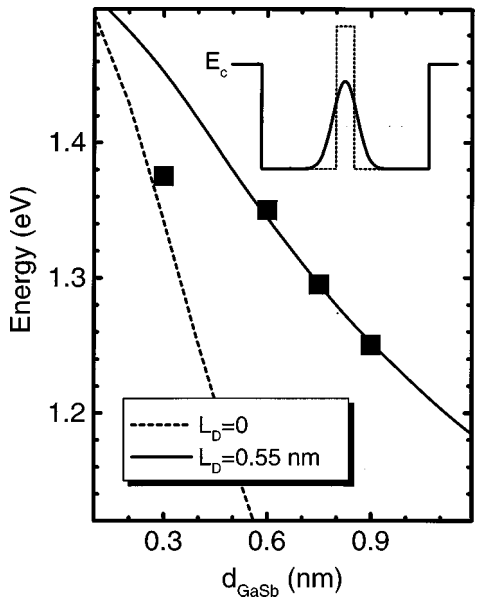

FIG. 5. Dependence of PL peak energy on GaSb layer thickness. Solid (dashed) line shows calculated electron heavy-hole transition energy for GaSb/GaAs quantum wells with (without) Sb diffusion. The inset shows the conduction-band profile with (without) diffusion using the same line styles.

WL transition appears at essentially the same energy as for the 0.9 nm sample. The quantum dot PL line has a FWHM of 100 meV, which is attributed to the relatively large dot size distribution already observed in the TEM pictures. The surprisingly large FWHM for the 0.9 nm nominal thickness is explained by the onset of QD formation.

The dependence of the peak energy of the GaSb-related luminescence on the average GaSb layer thickness recorded at 2 K and 5 W cm^{-2} is shown in Fig. 5 together with calculated energies for the heavy-hole transitions.[17] The calculated energies represent upper values since thermalization effects are not considered. It can be seen that for layer thicknesses larger than 0.3 nm, the calculated energies are below the experimentally observed ones. This disagreement can be explained by interface broadening due to an exchange reaction between Sb and As.[18–20] The resulting reduction of the minimum of the binding potential causes an increase in the transition energy.

Good agreement with the experimental data for nominal thickness 0.6, 0.75, and 0.9 nm is obtained when an antimony diffusion length L_D of about 0.55 nm is assumed (Fig. 5). The inset shows the profile of the conduction band with diffusion (solid line) and without (dotted line). The deviation for the 0.3-nm sample may be explained by larger uncertainty of the thickness or thermalization effects.

It can be assumed that in the 1.2-nm sample the remaining 0.3 nm of the GaSb is transformed into QD's. To simplify the calculation we assume a disk shape for the dots. A dot density of 4×10^{10} cm^{-2} corresponds then to an average GaSb dot height of 2.9 nm ($L_D=0$). For a 2.9-nm GaSb/GaAs disk and a Sb diffusion length of about 1 nm the QD luminescence energy of 1.08 meV can be modeled. Figure 6 shows the band alignment, wave functions, and energy levels for a 2.9-nm GaSb/GaAs disk with an abrupt interface and a graded interface due to Sb diffusion.

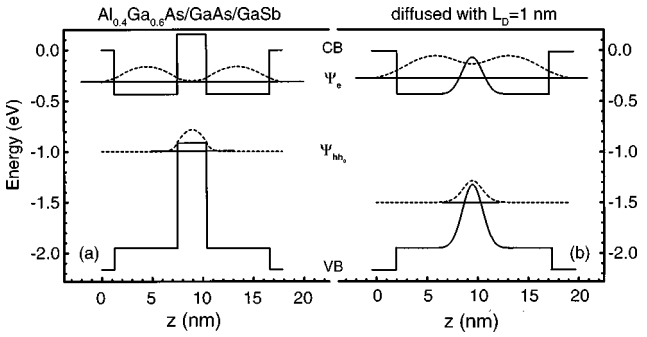

FIG. 6. Band alignment scheme for a 2.9-nm GaSb/GaAs disk with (a) an abrupt and (b) a graded interface due to Sb diffusion.

In Fig. 7 the PL spectra for different excitation energies and PLE spectra for different detection energies are shown. It is obvious that there seems to be only little ''communication'' between WL and QD's. It is almost impossible to excite QD luminescence by resonantly exciting the WL. Both QD and WL seem to be fed from the same states having an energy of 1.3 eV or greater. These results clearly show the different origin of the QD and WL luminescence lines and suggest that the luminescence of wetting-layer states in the 1.2-nm QD sample stems actually from localized states.

D. Excitation density dependent PL

Figure 8 shows the photoluminescence spectra of GaSb QD's recorded at different excitation densities between $0.01-500\ \mathrm{W/cm^2}$ ($T=5$ K) on a semilogarithmic scale. The low-energy PL line due to the QD's is dominant in the spectra at low-excitation density ($<0.5\ \mathrm{W/cm^2}$). With increasing excitation density, the PL peaks shift toward higher energies. This blueshift reflects the dipole layer formation caused by spatial separation of nonequilibrium holes confined in GaSb and electrons confined in the nearby GaAs region and is proportional to the third root of the excitation density $D^{1/3}$.[3,6,17] In Fig. 9 we show the dependence of the PL maximum (solid symbols) of the wetting layer and QD's on excitation density. The dashed lines show fits to the third root of the excitation density with the same proportionality constant. At excitation densities larger than $2.5\ \mathrm{W/cm^2}$ the PL maximum energies of QD's are systematically above the dashed line. This effect is due to the participation of an excited state (QD*) in the QD luminescence. The filling of the quantum dot density of states leads to an additional shift of the PL maximum energy to higher energies. The PL energies of the ground state of QD's, determined by a line-shape fit to the PL spectra, are shown also in Fig. 9 (open circles). The inset shows a PL spectrum at $250\ \mathrm{W/cm^2}$ and the corresponding fit. The position of the excited state of the QD is in accordance with the absorption spectrum. It can be seen that the ground state of QD's (open symbols in Fig. 9) continues to shift proportionally to $D^{1/3}$.

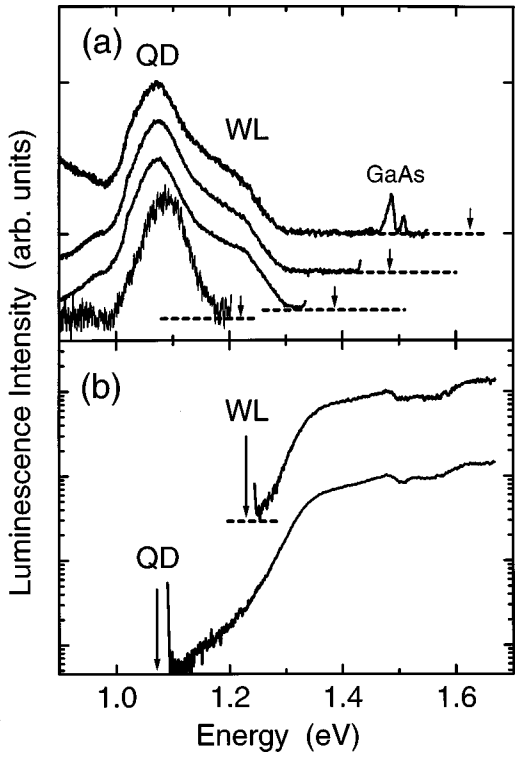

FIG. 7. (a) Selectively excited PL spectra (excitation energy is indicated by arrows) of 1.2-nm GaSb QD sample. (b) PLE spectra for detection energies on the QD and WL (marked by arrows). All measurements at $T=2$ K.

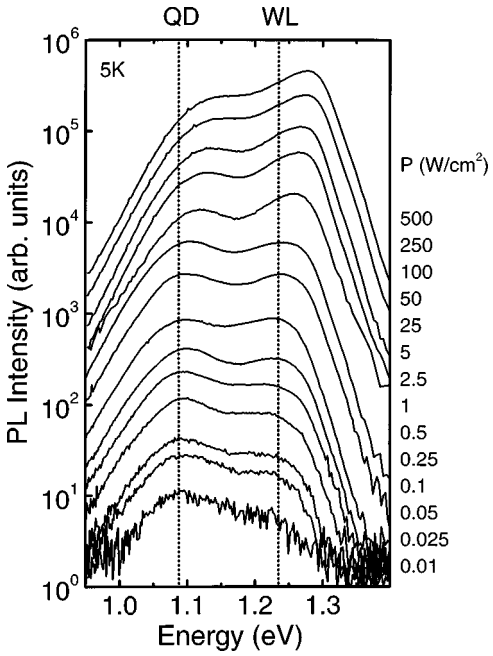

FIG. 8. PL spectra of the 1.2-nm GaSb structure ($T=5$ K) for different excitation densities between $0.01-500\ \mathrm{W/cm^2}$.

E. Oscillator strength

In order to investigate the dynamics of carrier recombination in GaSb QD's, we performed time-resolved CL measurements. Figure 10 shows the low-temperature (5 K) transients taken from the 1.2-nm GaSb QD sample at five different detection energies. The transients are strongly nonexponential.

In order to understand the decay we must take into consideration the dependence of electron-hole overlap on the nonequilibrium carrier density due to the band-bending effect in a type-II system. The static electric field of the array

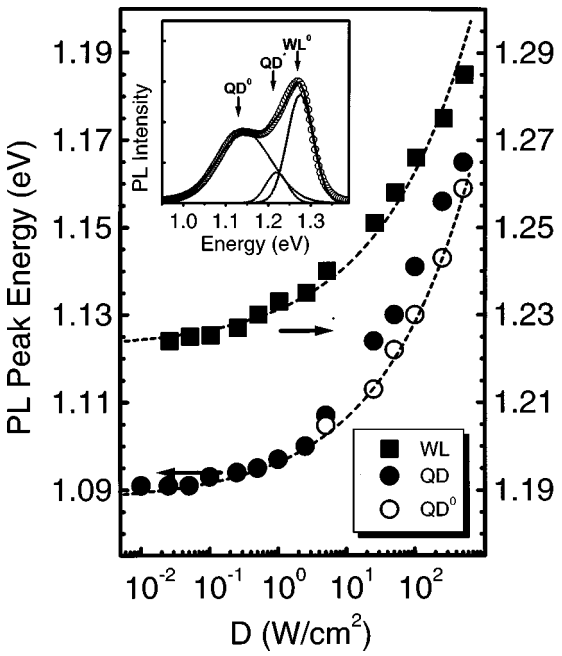

FIG. 9. Dependence of PL peak energy on excitation density for the wetting layer (square) and quantum dots (solid circle) of the 1.2-nm GaSb/GaAs sample. Dashed lines represent $D^{1/3}$ dependence with the same proportionality constant but different offset energy. The open circles represent the energy of the QD ground state as obtained from line-shape fits. The inset depicts the PL spectrum at $D=250$ W/cm^2 and the corresponding fit.

of positively charged dots will attract electrons in the GaAs barrier. The generated carriers recombine continuously and thus the electron-hole overlap decreases with time. After recombination of the majority of nonequilibrium carriers the band-bending effect is negligible, leading to a well-defined

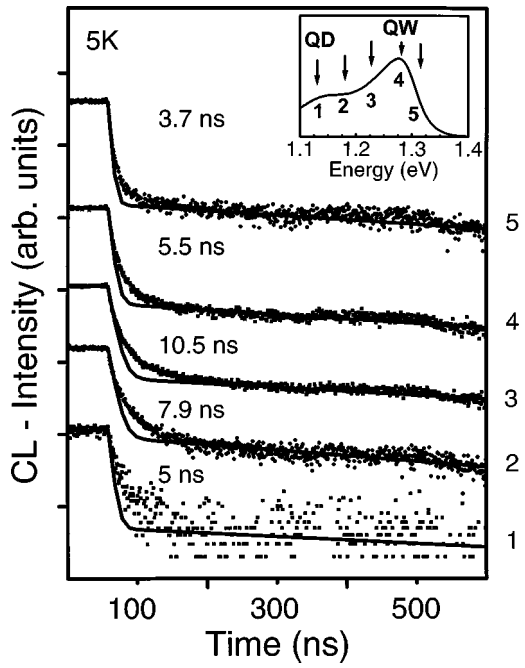

FIG. 10. Cathodoluminescence transients from 1.2-nm GaSb sample ($T=5$ K). The inset shows the CL spectrum with the positions of the detection energies marked by arrows.

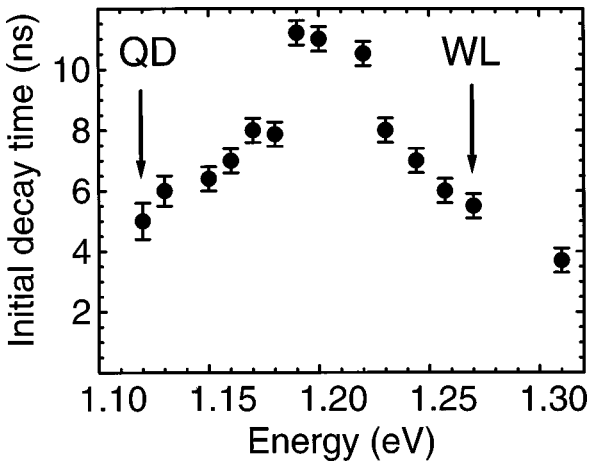

FIG. 11. Dependence of the initial decay time τ_1 on detection energy for the 1.2-nm GaSb sample.

decay time for a small average population. To simplify, we fit the transients with the sum of two exponential functions, corresponding to the initial (τ_1) and final (τ_2) decay constants. The fits of the experimental data are shown as lines with the short time constant τ_1 also in Fig. 10. The initial decay time in dependence on energy varies between 3.5 and 11 ns. In Fig. 11 we show the dependence of the initial decay time τ_1 on detection energy. These measurements suggest that the initial decay time τ_1 of the dots and the wetting layer are almost *equal*. The time constant τ_1 is $\tau_1(\mathrm{QD})=5\pm0.6$ ns and $\tau_1(\mathrm{WL})=5.5\pm0.4$ ns for QD and WL, respectively. We speculate that in between (around 1.2 eV detection energy) τ_1 is increased due to a smaller oscillator strength of excited QD states.

A small exciton binding energy and oscillator strength for type-II spherical QD's was predicted in Ref. 10. For a single

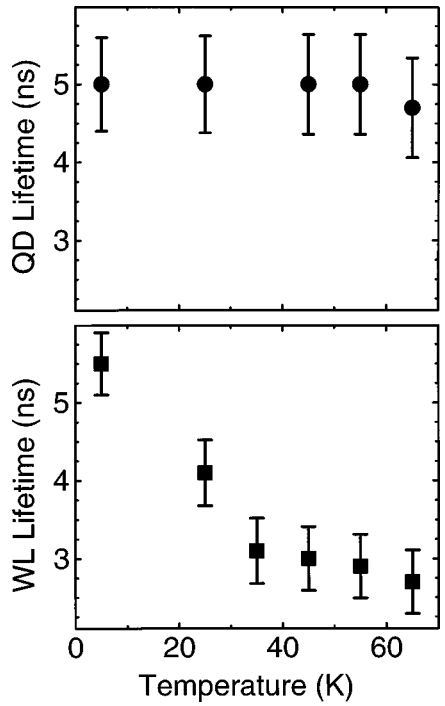

FIG. 12. Temperature dependence of the initial decay time for the QD and WL cathodoluminescence.

spherical GaSb quantum dot with the same volume as in our case, a very small electron-hole overlap $\ll 0.1$ is expected. In contrast, our results demonstrate large oscillator strength. If we assume an electron-hole overlap of 100% for an ideal type-I quantum dot and a carrier lifetime of about 2 ns as observed for InAs/GaAs QD's,[21] we expect for the dots with a carrier decay time of 5 ns, an electron-hole overlap of about 60%. This strong oscillator strength of GaSb QD's can be explained by the shape of the dots and the actual sample structure with $Al_yGa_{1-y}As$ barriers on both sides of the GaSb/GaAs layer. The $Al_yGa_{1-y}As$ barriers confine the electrons close to the GaSb layer, similar to what has been found for $In_xAl_{1-x}As$/InP quantum wells.[22] The electron-hole overlap, therefore, is larger than in a QD sample without $Al_yGa_{1-y}As$ barriers. Furthermore in our samples, we study the dynamic behavior of a sheet of dots. We attribute the slow decay constant (τ_2) of about 600 ns to recombination from separated, individual electron-hole pairs; it corresponds to a much smaller wave-function overlap of about 6%. To obtain a realistic estimate of the oscillator strength, in subsequent studies realistic sample geometries and carrier densities will be considered for model calculations.

As opposed to a type-I quantum dot, in the case of a GaSb quantum dot the electrons are localized in the two-dimensional GaAs, surrounding the positively charged GaSb region. For this reason the electrons are equally available for quantum dots and the wetting layer. This explains the similar decay time for both QD's and the WL. Figure 12 shows the temperature dependence of decay time for QD's and the wetting layer. The measurements are carried out between 5 and 65 K. The QD initial decay time is independent of the temperature in the measured range $T \leqslant 65$ K (about 5 ± 1 ns) as expected for well-localized zero-dimensional carriers. The decay time for the WL decreases with increasing temperature from 5.5 ns at 5 K to 2.5 ns at 65 K. Since simultaneously the WL luminescence intensity decreases, we suspect a nonradiative mechanism, possibly evaporation of holes out of the WL quantum well.

IV. CONCLUSION

The optical properties of and carrier dynamics in type-II $Ga_zSb_{1-z}As$/GaAs quantum dots have been investigated. Interband absorption from type-II quantum dots has been measured and coincides with the photoluminescence transition energies. (Sb,As) intermixing with an antimony diffusion length of about 1 nm is found to make an important contribution to the observed transition energies of wetting layer and quantum dot luminescence. Both dipole layer formation and quantum dot state filling contribute to the luminescence blueshift with increasing excitation density. At moderate carrier densities, of several excitons per dot, fast decay times of 5 ns are found suggesting wave-function overlap similar to type-I systems. At low carrier densities, large decay times in the order of 1 μs are found as expected for isolated, spatially indirect excitons.

ACKNOWLEDGMENTS

This work has been supported by Deutsche Forschungsgemeinschaft in the framework of Sfb 296, Volkswagenstiftung, and INTAS. One of us (N.N.L.) is grateful to the Alexander von Humboldt-Stiftung.

*On leave from A. F. Ioffe Physical-Technical Institute, St. Petersburg, Russia.

†Present address: Lawrence Berkeley Laboratory, University of California, Berkeley, California 94720.

[1] N. Kirstaedter, N. N. Ledentsov, M. Grundmann, D. Bimberg, V. M. Ustinov, S. S. Ruvimov, M. V. Maximov, P. S. Kop'ev, Zh. I. Alferov, U. Richter, P. Werner, U. Gösele, and J. Heydenreich, Electron. Lett. **30**, 1416 (1994).

[2] E. T. R. Chidley, S. K. Haywood, R. E. Mallard, N. J. Mason, R. J. Nicholas, P. J. Walker, and R. J. Warburton, Appl. Phys. Lett. **54**, 1241 (1989).

[3] F. Hatami, N. N. Ledentsov, M. Grundmann, J. Böhrer, F. Heinrichsdorff, M. Beer, D. Bimberg, S. S. Ruvimov, P. Werner, U. Gösele, J. Heydenreich, U. Richter, S. V. Ivanov, B. Ya. Meltser, P. S. Kop'ev, and Zh. I. Alferov, Appl. Phys. Lett. **67**, 656 (1995).

[4] P. M. Thibado, B. R. Bennett, M. E. Twigg, B. V. Shanabrook, and L. J. Whitman, J. Vac. Sci. Technol. A **14**, 885 (1996).

[5] B. R. Bennett, R. Magno, and B. V. Shanabrook, Appl. Phys. Lett. **68**, 505 (1996).

[6] E. R. Glaser, B. R. Bennett, B. V. Shanabrook, and R. Magno, Appl. Phys. Lett. **68**, 3614 (1996).

[7] T. Utzmeier, P. A. Postigo, J. Tamayo, R. García, and F. Briones, Appl. Phys. Lett. **69**, 2674 (1996).

[8] B. R. Bennett, B. V. Shanabrook, and R. Magno, Appl. Phys. Lett. **68**, 958 (1996).

[9] M. E. Rubin, H. R. Blank, M. A. Chin, H. Kroemer, and V. Narayanamurti, Appl. Phys. Lett. **70**, 1590 (1997).

[10] U. E. H. Laheld, F. B. Pedersen, and P. C. Hemmer, Phys. Rev. B **52**, 2697 (1995).

[11] C.-K. Sun, G. Wang, J. E. Bowers, B. Brar, H.-R. Blank, H. Kroemer, and M. H. Pilkuhn, Appl. Phys. Lett. **68**, 1543 (1996).

[12] D. Bimberg, T. Wolf, and J. Böhrer, in *Advances in Nonradiative Processes in Solids*, edited by B. di Bartolo (Plenum, New York, 1991), p. 577.

[13] D. Bimberg, H. Münzel, A. Steckenborn, and J. Christen, Phys. Rev. B **31**, 5490 (1985); J. Christen, Festkoerperprobleme **30**, 39 (1990).

[14] S. Ruvimov, P. Werner, K. Scheerschmidt, J. Heydenreich, U. Richter, N. N. Ledentsov, M. Grundmann, D. Bimberg, V. M. Ustinov, A. Yu. Egorov, P. S. Kop'ev, and Zh. I. Alferov, Phys. Rev. B **51**, 14 766 (1995).

[15] M. Grundmann, J. Christen, N. N. Ledentsov, J. Böhrer, D. Bimberg, S. S. Ruvimov, P. Werner, U. Richter, U. Gösele, J. Heydenreich, V. M. Ustinov, A. Yu. Egorov, A. E. Zhukov, P. S. Kop'ev, and Zh. I. Alferov, Phys. Rev. Lett. **74**, 4043 (1995).

[16] *Physics of Group IV Elements and III-V Compounds*, edited by O. Madelung, M. Schulz, and H. Weiss, Landolt-Börnstein Numerical Data and Relationships, New Series, Group III, Vol. 17, pt. a (Springer, Berlin, 1982).

[17] N. N. Ledentsov, J. Böhrer, M. Beer, F. Heinrichsdorff, M. Grundmann, D. Bimberg, S. V. Ivanov, B. Ya. Meltser, S. V. Shaposhnikov, I. N. Yassievich, N. N. Faleev, P. S. Kop'ev, and Zh. I. Alferov, Phys. Rev. B **52**, 14 058 (1995).

[18] M. Yano, M. Ashida, A. Kawaguchi, Y. Iwai, and M. Inoue, J. Vac. Sci. Technol. B **7**, 199 (1989).

[19] M. Yano, H. Yokose, Y. Iwai, and M. Inoue, J. Cryst. Growth **111**, 609 (1991).
[20] J. A. Dura, A. Vigliante, T. D. Golding, and S. C. Moss, J. Appl. Phys. **77**, 21 (1994).
[21] R. Heitz, M. Veit, N. N. Ledentsov, A. Hoffmann, D. Bimberg, V. M. Ustinov, P. S. Kop'ev, and Zh. I. Alferov, Phys. Rev. B **56**, 10 435 (1997).
[22] R. Zimmermann and D. Bimberg, J. Phys. IV **3**, C261 (1993).